

Structure and Physical Properties of (TMEO-TTP)₂Au(CN)₂

Takehiko MORI,* Hiroo INOKUCHI, Yohji MISAKI,[†] Hiroyuki NISHIKAWA,[‡]
Tokio YAMABE,^{‡*} Hatsumi MORI,^{††} and Shoji TANAKA^{††}

Institute for Molecular Science, Okazaki 444

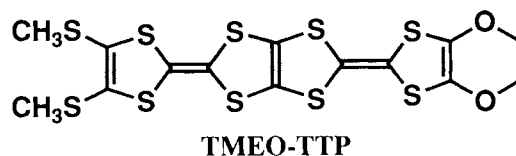
[†]Department of Molecular Engineering, Kyoto University, Yoshida, Kyoto 606

^{††}International Superconductivity Technology Center, Mutsuno, Nagoya 456

Radical cation salts of TMEO-TTP with linear and octahedral anions exhibit metallic conductivity down to 0.6 K. The title salt has two-dimensional donor arrangement, and the measurements of electrical conductivity, thermoelectric power, and ESR show a characteristic metal-to-metal transition.

Recently Misaki *et al.* have developed a general synthetic route to a new series of organic electron donors, BDT-TTP (2,5-bis(1',3'-dithiol-2'-ylidene)-1,3,4,6-tetrathiapentalene),¹⁾ and have found that some of their radical cation salts show high electrical conductivity.^{2,3)} In the present paper, we report radical cation salts of TMEO-TTP (2-(4',5'-bis(thiomethyl)-1',3'-dithiol-2'-ylidene)-5-(4'',5''-ethylenedioxy-1'',3''-dithiol-2''-ylidene)-1,3,4,6-tetrathiapentalene) (see below). Many of its salts exhibit metallic conductivity down to ³He temperatures. In particular we present a detailed investigation (*i.e.* crystal structure, thermoelectric power, and ESR) of (TMEO-TTP)₂Au(CN)₂.

Single crystals of the radical cation salts of TMEO-TTP²⁾ were prepared by electrochemical crystallization in 1,1,2-trichloroethane or THF in the presence of tetrabutylammonium salts of various



anions. As listed in Table I, linear anions (AuI₂, AuBr₂, Au(CN)₂) and octahedral anions (PF₆, AsF₆, and SbF₆) gave metallic salts; they showed high electrical conductivity 100-400 Scm⁻¹ at room temperature, and retained metallic conductivity down to 0.6 K (Fig. 1), though no superconductivity was observed down to this temperature. These anions also occasionally gave semiconducting salts even at room temperature.⁴⁾ Other tetrahedral (ClO₄, ReO₄, and BF₄) and monoatomic (Cl and Br) anions gave semiconducting salts.

Conducting behavior of (TMEO-TTP)₂Au(CN)₂ is exceptional among the salts of linear anions. At room temperature its conductivity is typically 200 Scm⁻¹ and weakly metallic, but in a cooling run the resistivity increases with several resistance jumps between 200 K and 100 K. Below 100 K there appears a metallic behavior with steep temperature dependence. In a heating run, there is no hysteresis up to 100 K, but the resistivity makes a maximum at around 180 K, and

Table 1. Composition and single-crystal conductivity of (TMO-TTP) A_x

Anion	Solvent	Form ^{a)}	$x^{b)}$	σ_{rt} /Scm ⁻¹	E_a /eV
AuI ₂	TCE, ^{c)} THF	N	0.63(Au) ^{d)}	100	Metallic down to 0.6 K
AuBr ₂	THF	P	0.23(Au), 0.24(Br)	300	Metallic down to 0.6 K
AuBr ₂	THF	N	0.68(Au), 0.70(Br)	0.12	0.1
Au(CN) ₂	TCE, THF	N	0.46(Au), 0.50(X)	200	Metallic down to 0.6 K ^{e)}
ClO ₄	TCE	N	1.2(Cl)	3	0.03
ReO ₄	TCE	N	0.69(Re)	0.12	0.04
BF ₄	TCE	N		0.5	0.05
PF ₆	TCE, THF	N	0.66(P)	150	Metallic down to 1.2 K
PF ₆	TCE	P	0.52(P)	200	Metallic down to 0.6 K
AsF ₆	TCE	N	0.52(As)	370	Metallic down to 0.6 K
SbF ₆	THF	P	0.25(Sb)	170	Metallic down to 0.6 K
SbF ₆	THF	N	0.36(Sb)	26	T_{MI} = 180 K
SbF ₆	TCE	P	1.0(Sb)	9	0.013
Cl	PhCN	N		0.005	0.15
Br	THF	N	0.82(Br)	0.01	0.15

a) N=needles, P=plates. b) Determined by the energy dispersion spectroscopy from the ratio of sulfur and the elements designated in the parentheses. X represents the value determined from the single crystal X-ray structure analysis. c) 1,1,2-trichloroethane. d) (TMO-TTP)(AuI₂)_{0.63}(I₃)_{0.18}. e) See Fig. 2.

decreases above this temperature (Fig. 2). The same behavior was observed for different four crystals. Though such a behavior may occur due to crystal cracks, it may be associated with the anomaly observed by the ESR measurement (vide infra).

The crystal structure of (TMO-TTP)₂Au(CN)₂ is depicted in Fig. 3.⁵⁾ The donors form conducting sheet along the ac plane, and the donor arrangement is similar to (BEDT-TTF)₂(ClO₄)(TCE)_{0.5} (BEDT-TTF:bis(ethylenedithio)tetrathiafulvalene),⁶⁾ where neighboring molecules of one donor molecule exist in the directions of about 0° (p1, p2), 30° (a1, a2), and 60° (c) from its molecular plane. All already reported BEDT-TTF salts with this type structure have semimetallic Fermi surface, which consists of small pieces of hole and electron pockets. The Fermi surface of the present salt is, however, rather metal-like than semimetal-like (Fig. 4);⁷⁾ the Fermi surface is connected along the a axis. This is because the donors form a "uniform stack" along the c direction (Fig. 3(b)), whereas the usual "ClO₄-type" BEDT-TTF salts have two-fold repeating unit along this "60° direction". Thus the Fermi surface of the present salt becomes to be open perpendicularly to this uniform direction (c axis).

Because the band structure is metal-like, the thermoelectric power (Seebeck coefficient) is positive in the whole temperature range (Fig. 2). On the contrary thermoelectric power of many semimetallic salts crosses zero at some temperature. It is, however, characteristic of the present salt that the thermoelectric power is relatively small (<5 μ V/K) over all temperatures. The thermoelectric power makes a broad maximum around 180 K, which corresponds with the temperature of the resistance maximum. The thermoelectric power showed no considerable hysteresis in cooling and heating runs.

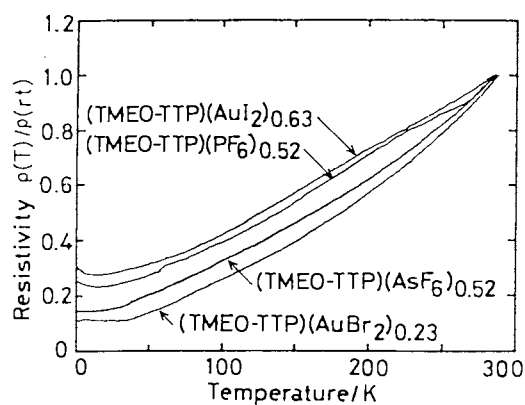


Fig. 1. Electrical resistivity of the metallic TMO-TTP salts.

(a)

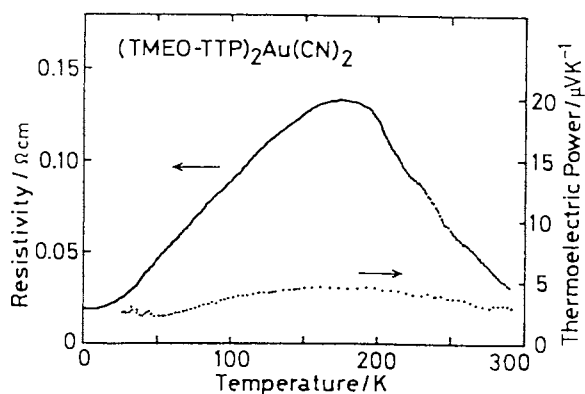
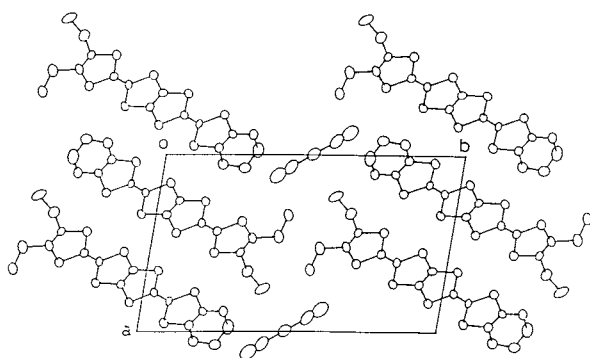


Fig. 2. Electrical resistivity (in a heating run) and thermoelectric power of $(\text{TMO-TTP})_2\text{Au}(\text{CN})_2$, measured along the c (needle) axis.

(b)

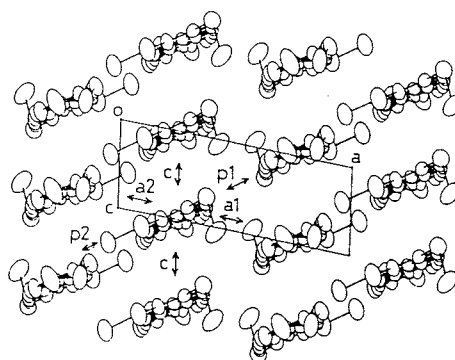


Fig. 3. Crystal structure of $(\text{TMO-TTP})_2\text{Au}(\text{CN})_2$; (a) projection onto the ab plane, and (b) arrangement of the donor sheet viewed along the donor molecular long axis.

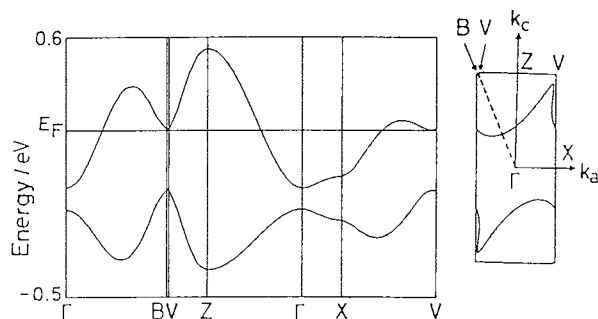


Fig. 4. Energy band and Fermi surface of $(\text{TMO-TTP})_2\text{Au}(\text{CN})_2$. The intermolecular overlap integrals are $c=4.2$, $a_1=18.3$, $a_2=7.3$, $p_1=-11.5$, and $p_2=-9.7 \times 10^{-3}$.

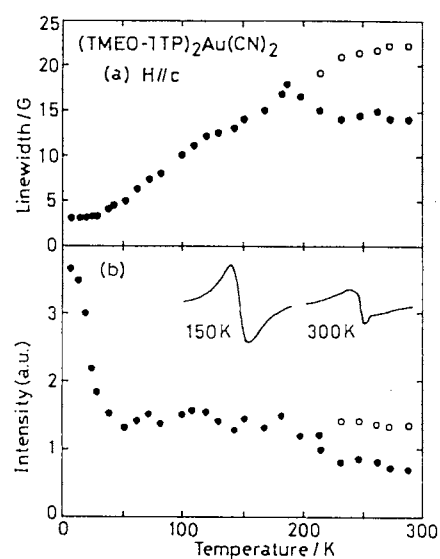


Fig. 5. (a) Peak-to-peak linewidth and (b) intensity of ESR of $(\text{TMO-TTP})_2\text{Au}(\text{CN})_2$.

The results of ESR are shown in Fig. 5. Except the Curie-like contribution of impurity at low temperatures, the intensity is almost constant, in consistent with the metallic conduction. The signal is symmetrical Lorentzian, the linewidth changes linearly to temperature, and the g value does not depend on temperature. Though the ESR signal splits to two above 200 K,⁸⁾ the total intensity (open circles in Fig. 5) seems to be kept unchanged even above this temperature. These two peaks, together with the anomalous behavior of the resistivity, can be explained if we assume the existence of two metallic phases; the low-temperature phase has higher resistance, and the mutual transformation between these phases is very slow. In view of the calculated Fermi surface, two-fold modulation along the c axis is a possible origin of the low-temperature phase. More detailed study of this phase transformation is underway.

This work was partly supported by Grant-in Aid for Scientific Research (No. 04640464) from the Ministry of Education, Science, and Culture.

References

- 1) Y. Misaki, H. Nishikawa, K. Kawakami, S. Koyanagi, T. Yamabe, and M. Shiro, *Chem. Lett.*, **1992**, 2321.
- 2) Y. Misaki, H. Nishikawa, T. Yamabe, T. Mori, H. Inokuchi, H. Mori, and S. Tanaka, *Chem. Lett.*, **1993**, 729.
- 3) T. Mori, H. Inokuchi, Y. Misaki, H. Nishikawa, T. Yamabe, H. Mori, and S. Tanaka, *Chem. Lett.*, **1993**, 733.
- 4) Crystal structure of semiconducting (TMO-TTP)AuBr₂(THF) will be reported in a separate paper.
- 5) Crystal data of (TMO-TTP)₂Au(CN)₂: triclinic, space group $P\bar{1}$, $a=11.535(3)$, $b=19.466(4)$, $c=4.825(1)$ Å, $\alpha=92.60(2)$, $\beta=90.64(2)$, $\gamma=98.88(2)^\circ$, $V=1069.1(4)$ Å³, and $Z=1$. Intensities were measured by the θ - 2θ scan technique on a Rigaku automated four-circle diffractometer AFC-5R with graphite monochromatized Mo K α radiation ($2\theta < 55^\circ$). After absorption correction, the structure was solved by the direct method and refined by the block-diagonal least squares procedure ($R = 0.057$, $R_w = 0.063$) by using 1827 independent reflections ($|F_o| > 3\sigma(F)$). Anisotropic thermal parameters were adopted for all non-hydrogen atoms.
- 6) H. Kobayashi, A. Kobayashi, Y. Sasaki, G. Saito, T. Enoki, and H. Inokuchi, *J. Am. Chem. Soc.*, **105**, 207 (1983).
- 7) The MO calculation was carried out by the extended Hückel method with using the parameters listed in T. Mori, A. Kobayashi, Y. Sasaki, H. Kobayashi, G. Saito, and H. Inokuchi, *Bull. Chem. Soc. Jpn.*, **57**, 627 (1984). By using the intermolecular overlap integrals of the HOMO, the band structure and the Fermi surface were calculated by the tight-binding approximation.
- 8) This occurred along all field directions, and in all examined samples. Interestingly there was observed no hysteretic behavior in the ESR.

(Received September 13, 1993)